

Investigation of space charge effects and matching of the proton beam for the in-vitro stage of LhARA

Theo Keseman

Abstract—In the process of designing the first stage (in vitro stage) of the Laser-hybrid Accelerator for Radiobiological Applications (LhARA), a study of the beam dynamics was undertaken using GPT and MAD-x. The effects of space-charge were taken into account for the possible intensities allowed by this experiment. Plotting phase space and emittance enabled to see the evolution of the beam. It was found that bunch intensities near 10^9 particles are probably too high to be able to neglect space-charge. An attempt - which needs to be pursued - to match the first part of the beam in order to recover the behaviour observed at intensities of 10^6 particles without space charge effects was nevertheless started by changing the strength of the first two Gabor lenses. The numerical errors arising from the GPT simulation were investigated by calculating the percent error on the emittance when varying the number of mesh lines and by changing the routine used to calculate the effect of space charge. The second part focuses on the attempt to implement the 90 degrees bend that injects the proton into the in-vitro cell. Starting from a total of 12 quadrupoles and 2 dipoles, solutions that necessitate the use of 6 quadrupoles and 2 sector bends were found, allowing space to be saved. The matching was based on parameters such as the dispersion in x and y, and its derivatives as well as Twiss parameters. This simulation was however not done with space charge effects.

I. INTRODUCTION

IT is now recognised that, for certain types of cancers, proton therapy presents numerous advantages - including the amount of radiation exposed to healthy tissues and the smaller risk of developing secondary cancers - over traditional radiotherapy. [1] In this context, it is planned that the Laser-hybrid Accelerator for Radiobiological Applications (LhARA) will deliver proton beams of sufficient energy (~ 15 MeV for in vitro studies [2]) by harnessing the advantages of laser-driven sources. The first stage of LhARA (adapted for in vitro studies) consists in a laser, a capture system with 2 Gabor lenses, an upstream matching with 3 other Gabor lenses, and a 90 degrees vertical bend leading to the end station where the cells are irradiated. [2] Previous simulations using Geant4 enabled to begin the necessary analysis to choose the number of lenses, dipoles, and quadrupoles, as well as their positions and strengths. However, the particles were not interacting in these simulations. As the beam is at a relatively low energy, it was expected that space charge effects could not be neglected. Accordingly, an investigation using the General Particle Tracer (GPT) was undertaken. The beam dynamics was then studied by calculating emittance and producing phase space plots for different bunch intensities.

As the cells need to be irradiated from the bottom, it was necessary to envisage the design of a 90 degrees bend, constituted of dipoles and quadrupoles. The second goal of this project was then to reduce the number of magnets used

in the arc. This was examined using MAD-x (Methodical Accelerator Design). Finally, using the results on the effects of space charge, matching the first part of LhARA was begun using GPT.

II. METHOD AND THEORY

A. GPT simulation

The GPT package enables the study of the behaviour of charged particles in electromagnetic fields by its 3D particle tracking techniques. [3] It was used to generate data files organised in time or position step, with parameters such as the velocity and position of each particle or the electromagnetic field at every point occupied by a particle. GPT offers different space-charge models, two of which were used : the spacecharge3Dmesh routine (based on the use of a multi-grid solver and a non-equidistant mesh and Poisson's equation), and the spacecharge3D one (applying Lorentz transformations). These enabled the evaluation of numerical errors. Statistical errors were calculated by dividing the data in 5 and treating each set independently.

In order to keep the computational time minimal while testing different bunch intensities, 10 000 macroparticles were simulated with a total charge uniformly spread among them. Beam dynamics was investigated by plotting the 4D transverse emittance, as well as in x and y, and producing phase space plots (x' and y' being respectively the momentum in the x and y directions divided by the momentum in the z direction). As the initial particle distributions were cylindrically symmetric, this allowed us to keep track of symmetries and eventual code errors. Phase space plots have also the advantage of being useful if one wants to match the beam line later.

Here, RMS emittance was used. In the x direction, it is defined as :

$$\epsilon_x = \sqrt{\begin{vmatrix} \sigma_x \sigma_x & \sigma_x \sigma_{x'} \\ \sigma_{x'} \sigma_x & \sigma_{x'} \sigma_{x'} \end{vmatrix}} \quad (1)$$

where:

$$\sigma_x \sigma_x = \langle xx \rangle \quad (2)$$

$$\sigma_{x'} \sigma_{x'} = \langle x'x' \rangle \quad (3)$$

$$\sigma_x \sigma_{x'} = \langle xx' \rangle \quad (4)$$

and similarly in the y direction.

In case both planes are not independent, this can be generalised to the 4D transverse emittance, calculated as:

$$\epsilon = \sqrt{\begin{vmatrix} \sigma_x \sigma_x & \sigma_x \sigma_{x'} & \sigma_x \sigma_y & \sigma_x \sigma_{y'} \\ \sigma_{x'} \sigma_x & \sigma_{x'} \sigma_{x'} & \sigma_{x'} \sigma_y & \sigma_{x'} \sigma_{y'} \\ \sigma_y \sigma_x & \sigma_y \sigma_{x'} & \sigma_y \sigma_y & \sigma_y \sigma_{y'} \\ \sigma_{y'} \sigma_x & \sigma_{y'} \sigma_{x'} & \sigma_{y'} \sigma_y & \sigma_{y'} \sigma_{y'} \end{vmatrix}} \quad (5)$$

It is shown from Liouville's theorem [4] that emittance is a conserved quantity when the beam is travelling at constant speed. Hence, it is expected that emittance will remain constant when subject to negligible magnetic (outside the Gabor lenses here), non-linear effects taking place inside the magnets.

Space charge was first activated from the initial position of the beam. But it was soon realised that the initial beam being composed of both electrons and protons due to the laser hitting the target, it would be neutral which does not lead to any initial space charge effect. As a result, it was activated from 5 mm onwards to enable the electrons to get sufficiently ahead from the protons.

The five Gabor lenses were simulated with equivalent solenoids with the following currents ¹ : 7.31×10^5 A at $z = 0.579$ m and $z = 1.59$ m, 6.99×10^5 A at $z = 3.24$ m, 1.10×10^5 A at $z = 6.95$ m and 1.12×10^5 A at $z = 11.0$ m.

B. MAD-x simulation

The Methodical Accelerator Design (MAD-x) was used to match the 90 degrees bend that constitutes the final part of the in-vitro stage. This was done by setting constraints at the start and the end of the bend on the linear lattice functions. These come from the following solution of Hill's equation [5] ²:

$$x = \sqrt{\epsilon\beta(s)}\cos(\phi(s) + \phi_0) \quad (6)$$

where β is the amplitude function (corresponding to the envelope of the beam), ϵ is the emittance (taken to be constant as the beam is not accelerating), ϕ_0 is determined by initial conditions and ϕ is the phase advance, related to the amplitude function by:

$$\phi = \int \frac{ds}{\beta} \quad (7)$$

The phase advance was initially used in the middle of the bend to find a solution to match the beam with 10 quadrupoles and 2 dipoles.

From this, the correlation function is defined as:

$$\alpha = -\frac{1}{2} \frac{d\beta}{ds}, \quad (8)$$

Next, the dispersion of x and p_x are defined as:

$$D_x = \frac{\partial x}{\partial p_t}, D_{p_x} = \frac{1}{p_s} \frac{\partial p_x}{\partial p_t} \quad (9)$$

where $p_t = \Delta E/p_s c$.

When defining a sector bend, the length and the angle need to be specified. These correspond to the arc length of the reference orbit and the bend angle. For quadrupoles, a value for the normal quadrupole coefficient K_1 is also needed. It is defined as :

$$K_1 = \frac{1}{B\rho} \frac{\partial B_y}{\partial x} \quad (10)$$

¹These values correspond to one loop currents and can therefore be decreased.

²In the following, s is the axis determined by the tangent to the reference orbit in the local curvilinear coordinate system (x, y, s) with ρ being the distance to the centre of curvature.

with B_y being the magnetic field in the y direction. Hence, a positive quadrupole results in focusing the beam in the horizontal direction, and a negative coefficient results in focusing it in the vertical direction.

III. RESULTS AND ERRORS

A. Space charge effects

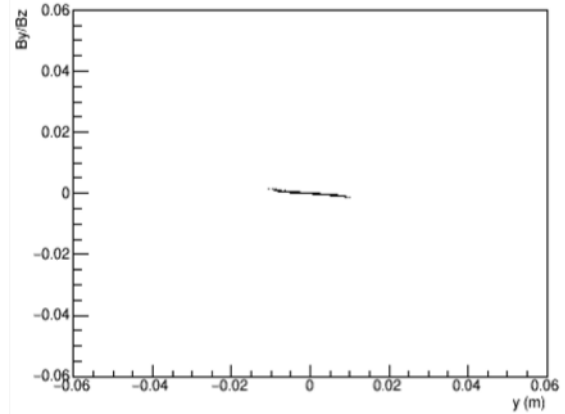


Fig. 1. Phase space plot in the y direction at $z = 13.24$ m for an intensity of 10^6 particles without space charge.

Space charge effects were tested by plotting phase space plots in x and y each 10^{-8} second from 0 to 25×10^{-8} s. This was done for bunch intensities of 10^6 , 10^7 , 10^8 and 10^9 particles with space charge effects activated from 5 mm, as well as for a bunch intensity of 10^6 particles without space charge activated. ³ As can be seen in Fig. 1 - 4, the simulation shows no difference with and without space charge up to an intensity of 10^7 particles. It seems also that a bunch intensity of 10^8 particles can be acceptable. However, the discrepancy

³Only a few example plots are shown here, see the attached files for the complete results.

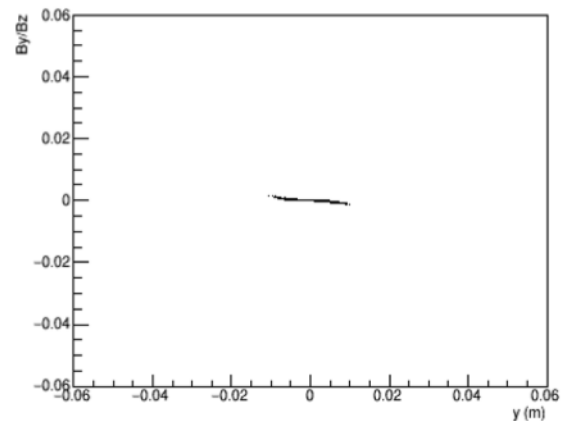


Fig. 2. Phase space plot in the y direction at $z = 13.24$ m with 10^7 particles with space charge.

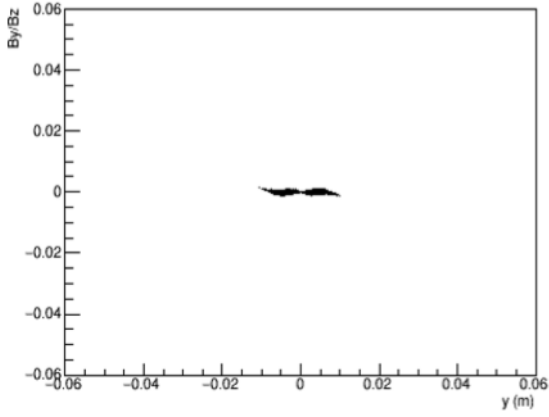


Fig. 3. Phase space plot in the y direction at $z = 13.24$ m with 10^8 particles with space charge.

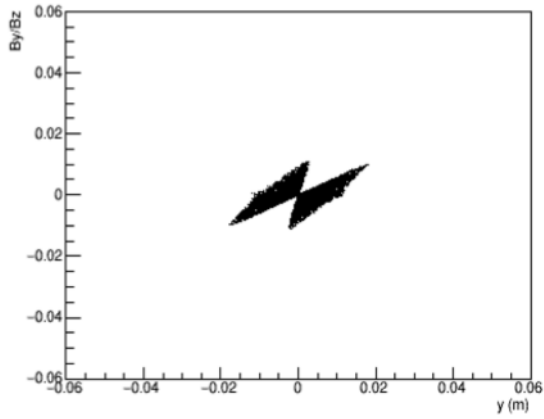


Fig. 4. Phase space plot in the y direction at $z = 13.24$ m with 10^9 particles with space charge.

with the simulation comprising 10^9 particles looks too great as, by matching the lenses, one can tilt the ellipse in the phase space or reduce its size but not change its shape in an obvious way. In addition, the discrepancy between 10^8 particles and less becomes mostly observable only after 10 meters, which also suggests that space charge effects are not yet too important

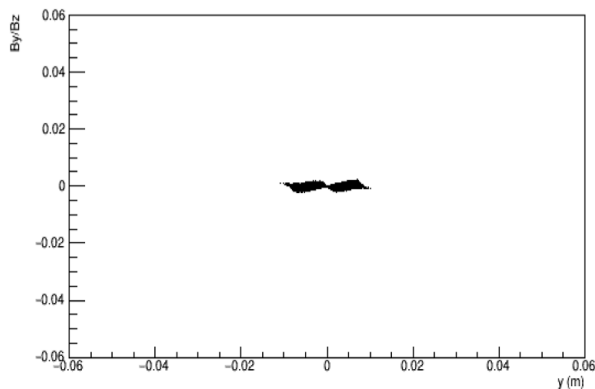


Fig. 5. Phase space plot in the y direction at $z = 13.24$ m with 5.10^8 particles with space charge.

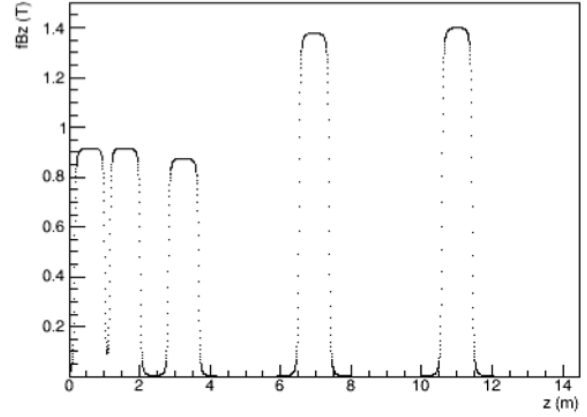


Fig. 6. Magnetic field in the z direction caused by the Gabor lenses along the beam

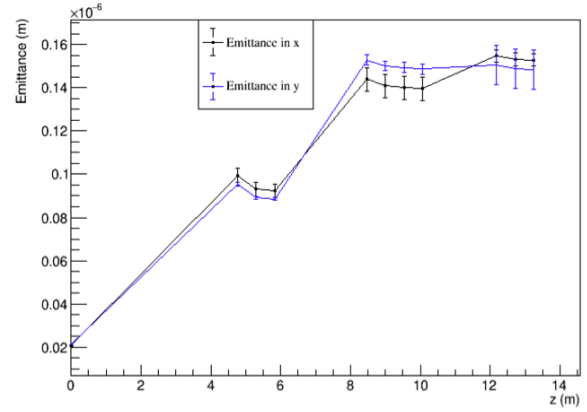


Fig. 7. Plot of the emittance at an intensity of 10^6 particles without space charge effects.

at this intensity. On the contrary, phase space plots with 10^9 particles starts to differ from the rest from 10^{-8} second. In order to know at what intensity space charge effects start to become too important, phase space plots at $t = 25.10^{-8}$ with totals of 2.10^8 and 5.10^8 particles were inspected. Fig. 5 shows the result in the second case. From this plot, it seems therefore that a bunch intensity of 5.10^8 particles might also be acceptable.

Since non-linear effects are not negligible inside the lenses, the emittance was additionally plotted but only the results in weak magnetic fields is shown in Fig. 7 - 8. Points were taken using Fig. 6, which shows the magnetic field in the z direction - that is, the magnetic field acting on a particle travelling on the reference orbit - across stage 1 (without the arc). As Fig. 6 reveals, the first two Gabor lenses are too close to consider the magnetic field negligible. The case concerning the space between the second and third lens is less evident. Emittance was plotted for $z = 2.4$ m and $z = 2.5$ m. It was found that for total charges of 10^6 and 10^7 , the emittance was 5 to 10 times bigger than for the other points, the strength of the magnetic field between the second and third lenses being an order of magnitude higher than between the third and fourth lenses.

These figures reveal first that the emittance in x and y are

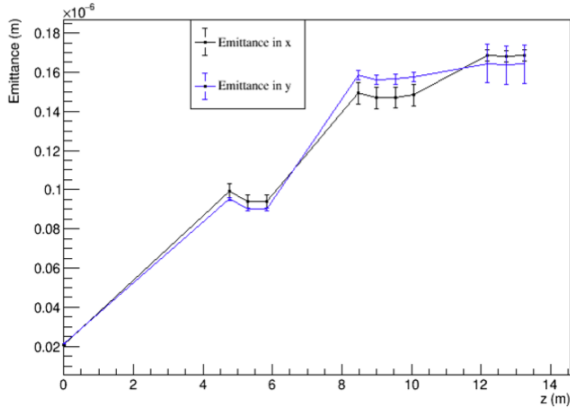


Fig. 8. Plot of the emittance at an intensity of 10^6 particles with space charge effects.

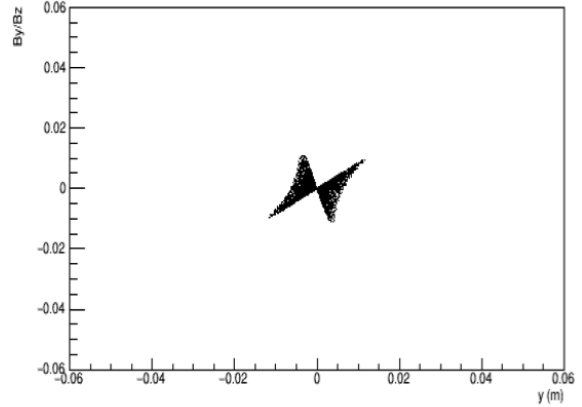


Fig. 10. Phase space plot in the y direction at $z = 12.7$ m with a 3.75 cm radius circular aperture with 10^9 particles.

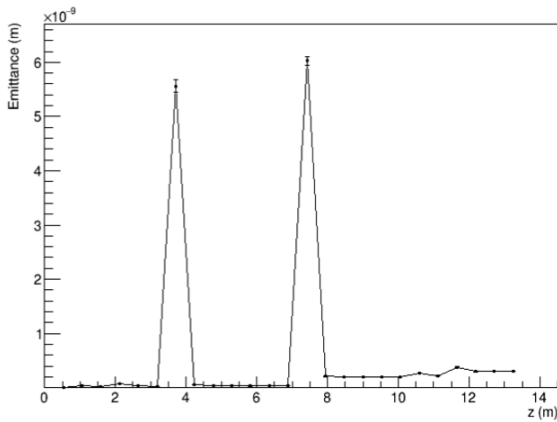


Fig. 9. Plot of the 4D transverse emittance at an intensity of 10^9 particles with space charge effects.

close even if they do not lie within the error bars of the emittance calculated in the other plane. This indicates that the cylindrical symmetry of the beam is not broken throughout the first stage up to the arc but the 4D transverse emittance, an example plot of which is illustrated in Fig. 9, did not reflect the same pattern. If there is emittance growth in the weak field regions, only two peaks are present whereas 3 appear when the emittance is plotted only in x or y for all magnetic fields present along stage 1.⁴ Emittance values show also for the first time a difference when space charge is activated or not for the same charge. Indeed, for the first case, it culminates at almost 0.17 m at $z = 13$ m when it only goes to 0.15 m without space charge effect. Generally, as the intensity increases, so does the emittance, bunch intensities of 10^8 and 10^9 particles leading respectively to an emittance of one and two orders of magnitude higher than for an intensity of 10^6 particles. Finally, a net emittance growth, which cannot be attributed to its dependence on magnetic fields, is observed for all intensities, the magnetic field being $2.45 \cdot 10^{-4}$ T, $2.14 \cdot 10^{-4}$ T and $1.16 \cdot 10^{-4}$ T at respectively $z = 5.0, 9.0, 13$ m.

The plots shown here are the result of setting a circular

⁴A clear discrepancy in the orders of magnitude also leads to think that an error lies in the code used but none was found.

aperture with a radius of 1 meter in order to keep track of all the particles in the first place, but particles will be physically lost. Simulations setting the radius to 3.65 cm were also done. While no particle was lost without space charge, it was found that 5148 particles out of the original 10000 were remaining after passing through the five Gabor lenses when 10^9 particles were simulated. The corresponding y phase space plot is shown in Fig. 10. In the case of a bunch intensity of 10^8 particles, 8721 were remaining at the end.

Secondly, the numerical accuracy of the GPT simulations was tested by varying the number of mesh lines as already mentioned. 100 mesh lines in both the x and y directions, as well as 250 in the z direction was taken as the reference number of mesh lines as, for time and/or memory limitations, it was not possible to run completely the simulation with a higher number of mesh lines. The proportion of mesh lines in the different directions and the total intensity of 10^8 particles were kept constant. When comparing the emittance in x with $100 \times 100 \times 250$ mesh lines, the results given by $40 \times 40 \times 100$, $60 \times 60 \times 150$, $80 \times 80 \times 200$ mesh lines differed respectively by 1.21 %, 0.753 % and 0.300 %. This was taken to be sufficiently precise, however a later simulation that did not use mesh lines and was presented by GPT as the "best with respect to the physics included" was produced. This was done for a bunch intensity of 10^8 particles with a 3.65 cm radius aperture. A 4.82 % discrepancy was found between this simulation and the $100 \times 100 \times 250$ mesh lines one.

Finally, an attempt to match the beam for an intensity of 10^9 particles in GPT was undertaken. The effect of reducing and increasing the magnetic field inside the first lens by 10 % and 50 % while leaving the second one unchanged and conversely was studied. It was found that changing the magnetic field by 10 % was not enough to obtain significant variations in the phase space plots. In addition to the eight possibilities generated in this way, the effect of setting the magnetic field to 1.00 T and 1.373 T in the first lens while keeping the second to 0.5 T was tested. The last combination enabled to get closer to the phase space observed without space charge at $t=3$ s, as evidenced by Fig. 11 - 13.

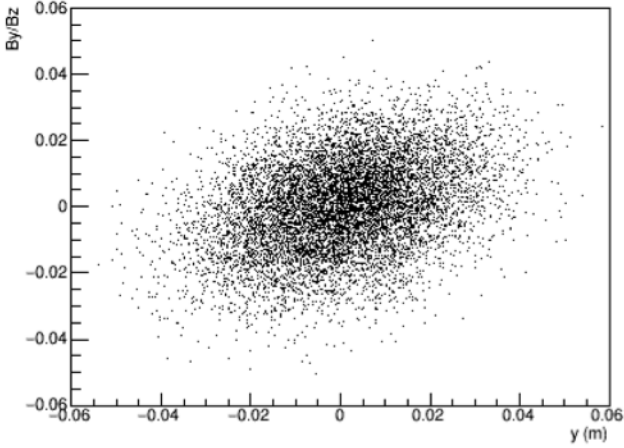


Fig. 11. Phase space plot in the y direction at $t = 3$ s with 10^6 particles without space charge effect.

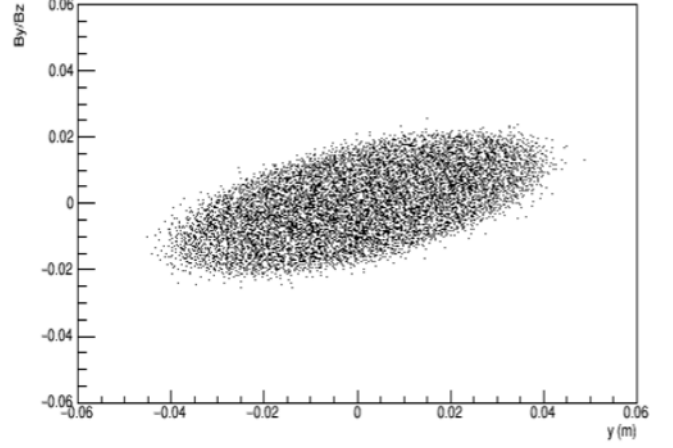


Fig. 13. Phase space plot in the y direction at $t = 3$ s with 10^9 particles with space charge effect and magnetic fields of 1.373 T and 0.5 T in the first 2 Gabor lenses.

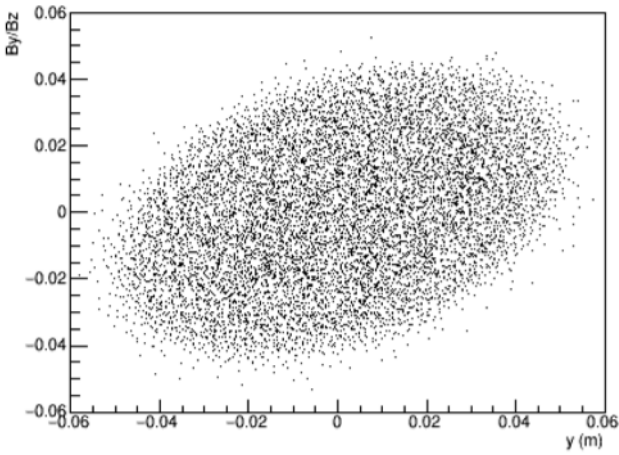


Fig. 12. Phase space plot in the y direction at $t = 3$ s with 10^9 particles with space charge effect.

	3 quadrupoles	4 quadrupoles
D1	0.1 m	0.1 m
<u>Sbend</u>	0 m ⁻²	0 m ⁻²
D2	0.15 m	0.1 m
Kqd1	-39.8116 m ⁻²	-27.2360 m ⁻²
D3	0.15 m	0.4 m
Kqf1	72.2927 m ⁻²	51.3056 m ⁻²
D4	0.5 m	0.1 m
Kqd2	-50.4514 m ⁻²	-33.1589 m ⁻²
D5	0.15 m	0.1 m
Kqf2	88.1044 m ⁻²	--
D6	0.4 m	--

Fig. 14. Summary of the values found for the drift spaces and quadrupoles while matching the beam for 6 and 8 quadrupoles. "D" stands for drift space length, "Kqd" is the defocusing quadrupole coefficient and "Kqf" is the focusing quadrupole coefficient.

B. Matching of the arc

The lengths of the magnets were chosen to be 45 cm for the sector bends and 6 cm for the quadrupoles. The amplitude and the correlation functions were set respectively to 300 m and 0 (as the beam should not start diverging in the cells) at the beginning and the end in both planes. The dispersion of x , y , p_x and p_y were also set 0. From the symmetry of the system, it was deduced that only half of the quadrupole coefficients needed to be specified, alternating defocusing and focusing quadrupoles in half an arc. The results that were obtained are summarised in the table above. To obtain the full line, one just has the reverse replace every quadrupoles in the opposite order. However, even though these combinations of quadrupoles give good agreement with the constraints imposed and reduce the total length of the arc to less than 3 meters (cf. Fig. 15), this simulation was done without space charge. This might have a big effect as the suggested solutions have both a focus point (the amplitude function being 0 in both planes simultaneously) as exhibited in Fig. 15 for the bend constituted of 6 quadrupoles.

IV. CONCLUSION

Space charge effects were studied for different bunch intensities. It was concluded that these may become too important for intensities neighbouring 10^9 particles. For each total charge tested, the emittance was growing. It was shown that this was not a result from the non-linear effects induced by the magnetic field. The number of lost particles was also examined when the size of the aperture was reduced. This was another argument to reject high bunch intensities as almost half of the particles were lost by the end of the transport. An attempt to match the beam for these intensities was still started. Setting the magnetic fields to 1.373 T and 0.5 T in the first and second lenses lead to a better agreement with the space phase plot done without space charge but matching the complete line is still necessary to conclude whether such intensities can be included in LhARA. The errors generated by the GPT were considered as well. While the difference in the results obtained with different numbers of mesh lines was relatively small, changing the routine gave results that were almost 5% off.

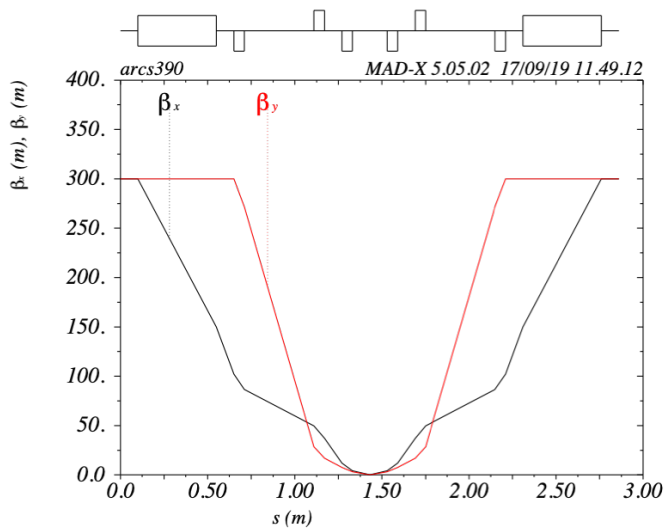


Fig. 15. Plot of the amplitude functions in x and y as a function of s.

Finally, the 90 degrees arc was matched with MAD-x, allowing the length of the bend to be reduced to less than 3 meters. However, the solution found will need to be implemented on GPT to evaluate the consequences of the focus present halfway through the arc.

REFERENCES

- [1] Levin W. P., Kooy H., Loeffler J. S., DeLaney T. F. (2005) *Proton Beam Therapy*. British Journal of Cancer. 93 (8): 849-854.
- [2] Kurup A., Pasternak J., Taylor R., et al. (2019) *Simulation of a radiobiology facility for the Centre for the Clinical Application of Particles*. European Journal of Medical Physics, vol. 65, 21-28.
- [3] Van der Geer S. B., De Loos M. J. *General Particle Tracer: User Manual*. Version 2.81, 12.
- [4] Barletta, Spentzouris and Harms (2012) US Particle Accelerator School Notes [online] Available at: <https://uspas.fnal.gov/materials/10MIT/Emittance.pdf>
- [5] Grote H., Schmidt F., Deniau L. (2016) *The MAD-x Program: User's Reference Manual* European Laboratory for Particle Physics. Geneva, Switzerland.